

Supplementary Information

**Functionalized polystyrene nanoplastics induced energy homeostasis
imbalance and immunomodulation dysfunction of marine clams
(*Meretrix meretrix*) at environmentally relevant concentrations**

Liuqingqing Liu^a, Hao Zheng^{a,b,*}, Liping Luan^a, Xianxiang Luo^{a,b,*}, Xiao Wang^{a,b},
Hui Lu^a, Yan Li^a, Liuying Wen^c, Fengmin Li^{a,b}, Jian Zhao^{a,b}

^a*Institute of Coastal Environmental Pollution Control, Frontiers Science Center for Deep
Ocean Multispheres and Earth System, Key Laboratory of Marine Environment and Ecology,
Ministry of Education, Ocean University of China, Qingdao 266100 China*

^b*Laboratory for Marine Ecology and Environmental Science, Qingdao National Laboratory for
Marine Science and Technology, Qingdao 266237, China*

^c*Tobacco Research Institute, Chinese Academy of Agricultural Science, Qingdao 266101,
China*

*Corresponding authors: zhenghao2013@ouc.edu.cn (Dr. Zheng);

lxx81875@ouc.edu.cn (Dr. Luo)

Name of the journal: *Environmental Science: Nano*

Date of the document prepared: May 11, 2021

Environmentally relevant concentrations of MPs and NPs

Determination of the clam ingestion rate and oxygen consumption rate

Number of pages: 22

Number of figures: 9

Number of tables: 4

Environmentally relevant concentrations of MPs and NPs

The exposure concentration of NPs (0.02–2.0 mg L⁻¹) in the present study was selected according to the reported and predicted environmentally relevant concentrations of MPs and NPs. As shown in Table S2, the reported abundance of MPs in seawater ranged 7.6×10⁻¹²–1.6×10⁴ mg L⁻¹. Weathering or ageing of a single MP particle can yield millions to billions of NPs.¹ Our previous study reported that the mass yield of PS NPs (~75.2 nm) from photodegradation (a common ageing process in marine ecosystem) of PS MPs (~38.6 μm) was 7.03 ± 0.37% (w%).² Accordingly, the estimated concentration of PS NPs in marine environment could be up to 5.3×10⁻¹⁰–1.1×10³ mg L⁻¹. In addition,³ predicted that the environmental concentration of NPs (50 nm) was 1.0×10⁻⁹–1.5×10⁻² mg L⁻¹ using a theoretical 3D fragmentation model. The highest predicted concentration of 0.015 mg L⁻¹ was at the same magnitude order of the lowest exposure concentration of 0.02 mg L⁻¹ used in this study. Moreover, the concentrations of NPs used in previous toxicological investigations ranged 0.1–100 mg L⁻¹ (Table S1). Therefore, to be environmentally relevant and comparable with previous studies, we selected 0.02, 0.2, and 2 mg L⁻¹ as the exposure concentrations of two NPs in the present study.

Determination of the clam ingestion rate and oxygen consumption rate

Ingestion rate, an indicator of feeding activity of clam,⁴ is defined as the quantity of microalgae ingested by per unit body weight of clams at given time.⁵ In order to determine the ingestion rate, one clam was randomly selected from each beaker after 7 days of exposure and maintained in a 500 mL glass beaker containing 400 mL filtered seawater. The clam was fed with the 2 × 10⁵ cells mL⁻¹ mixed algae of *C. meülleri* and

I. zhanjiangensis (1: 1, v/v). After 30 minutes of ingestion, 5 mL water sample was collected from the beak using pipette to determine the number of residual algae cells using a hemocytometer. The ingestion rate was calculated according to the following equation:

$$\text{Ingestion rate} = V \times (C_0 - C_T) / (W \times T) \quad (1)$$

where V (mL) is the volume of seawater, W (mg) is the dry weight of clam soft tissue, T (h) is the ingestion time of 30 minutes, C_0 and C_T (cells mL⁻¹) is the algae density at initial and T time during the ingestion, respectively.

For measuring the oxygen consumption rate, an indicator of metabolic rate,⁴ one clam was randomly selected from each beaker and was placed into a wild-mouth bottle with filtered full aeration seawater (dissolved oxygen 8.53 ± 0.05 mg L⁻¹). After 2 hours of cultivation at 17 °C in an illumination incubator (GXZ- 500C-LED, Ningbo, China), the content of dissolved oxygen in the seawater was measured by an oximeter (YSI-5000, Yellow Spring, Ohio, USA). Then the OCR was calculated as the following equation:

$$\text{Oxygen consumption rate} = (D_0 - D_T) / (W \times T) \quad (2)$$

where D_0 and D_T (mg) is the oxygen content at initial and T time; T (h) is the oxygen consumption time; W (mg) is the dry weight of clam soft tissue at time T .

Table S1. The summarized exposure concentrations of NPs in previous studies.

	Organisms	NP type	NP size (nm)	Exposure concentration (mg L ⁻¹)	Reference
Phytoplankton	Blue-green alga (<i>Microcystis aeruginosa</i>)	PS-NH ₂	200	0.5–7	6
	Microalgae (<i>Scenedesmus obliquus</i>)	PS	100, 500	1–100	7
	Cyanobacteria (<i>Synechococcus elongates</i>)	PS-NH ₂	100		
		PS	100	5	8
Zooplankton	Sea urchin embryo (<i>Paracentrotus lividus</i>)	PS-NH ₂	50	1–50	9
	Rotifer (<i>Brachionus koreanus</i>)	PS-COOH	40		
		PS	50, 500	10	10
	<i>Daphnia magna</i>	PS	100	1–75	11
	<i>Daphnia magna</i>	PS	100–120	1–400	12
	Brine shrimp (<i>Artemia franciscana</i>)	PS-NH ₂	50	0.1–10	13
	<i>Daphnia magna</i>	PS	20	1, 50	14
Bivalve	Blue mussel (<i>Mytilus edulis</i>)	PS	30	100–300	15
	Mussels <i>Mytilus galloprovincialis</i> (hemocytes)	PS-NH ₂	50	1–50	16
	Scallops (<i>Pecten maximus</i>)	PS	25, 250	0.015	17
	Pacific oysters (<i>Crassostrea gigas</i>) (gametes)	PS-NH ₂			
		PS-COOH	100	0.1–100	18
	Pacific oysters (<i>Crassostrea gigas</i>) (gametes)	PS	50, 500		
		PS-NH ₂	50	0.1–25	19
		PS-COOH	50		
	Blood clams (<i>Tegillarca granosa</i>)	PS	500	0.26	20
<i>C. fluminea</i>	PS	80	0.1–5	21	
Fish	Zebrafish	PS	25	10	22
	Zebrafish (<i>Danio rerio</i>)	PS	20-500	100	23
	Yellow croaker (<i>Larimichthys crocea</i>)	PS	100	5.50×10 ⁻¹² –5.50×10 ⁻⁷	24

Table S2. Reported abundance of MPs in global seawater.

Region	Reported concentration	Size (μm)	Normalized concentration (mg L^{-1}) ^a	Reference
North Pacific Central Gyre	$64\text{--}3\times 10^4 \text{ g km}^{-2}$	330–5000	$4\times 10^{-4}\text{--}2.0\times 10^{-1}$	25
Australian vessels	$9\times 10^3\text{--}1\times 10^5 \text{ particles km}^{-2}$	330–5000	$1.1\times 10^{-9}\text{--}4.7\times 10^{-2}$	26
South Pacific subtropical gyre	$71\text{--}732 \text{ g km}^{-2}$	330–5000	$5.0\times 10^{-4}\text{--}4.9\times 10^{-3}$	27
Kuril–Kamchatka Trench area	$60\text{--}2\times 10^3 \text{ particles m}^{-2}$	330–1000	$7.6\times 10^{-12}\text{--}7.3\times 10^{-6}$	28
Yangtze Estuary	$9.8\times 10^4\text{--}2.6\times 10^5 \text{ particles L}^{-1}$	330–5000	$1.9\times 10^{-7}\text{--}1.8\times 10^1$	29
Southeast coast of India	$10\text{--}30 \text{ particles L}^{-1}$	500–1000	$6.9\times 10^{-1}\text{--}1.6\times 10^1$	30
Gulf of Mannar	$6\text{--}223.6 \text{ particles L}^{-1}$	1000–5000	$3.3\text{--}1.6\times 10^4$	31
Hangzhou Bay	$100\text{--}500 \text{ particles L}^{-1}$	330–5000	$1.9\times 10^{-9}\text{--}3\times 10^{-4}$	32
Marmara Sea	$3\text{--}124 \text{ particles L}^{-1}$	50–5000	$2.1\times 10^{-5}\text{--}8.7\times 10^3$	33
South China Sea	$6.6\text{--}36.6 \text{ particles L}^{-1}$	330–5000	$1.0\times 10^{-4}\text{--}2.6\times 10^3$	34

^a Normalized concentration (mg L^{-1}) was calculated using the spherical volumes and density (1.04 g cm^{-3}) of polystyrene beads.³

Table S3. Histopathological alterations in the digestive gland of clams and their weight values.

Reaction pattern ^a	Histopathological alteration	Weight (w) ^a
Tubule alterations	Necrosis (nes)	3
	Epithelial cell hypertrophy (ech)	2
	Widening of the tubular lumen (wtl)	2
	Epithelial cell exfoliation (ece)	2
Intertubular tissue changes	Fibrosis (fis)	2
	Haemocytes infiltrate (hai)	1

^a Reaction pattern and weight values were classified according to previous studies.³⁵⁻³⁸ The alterations were classified into three weight (w) values according to the biological significance of the lesion, represented the degree in which the lesion might affect the normal function of the tissue or organ. Marked pathological (w = 3), the lesion was generally irreversible, leading to partial or total loss of the organ function. Moderate pathological (w = 2), the lesion was easily reversible in most cases if the stressor is neutralized. Minimal pathological (w = 1), the lesion was easily reversible as exposure to irritants ends.

Table S4. Differentially expressed genes of clams related to energy homeostasis and immunomodulation in the form of fragments per kilobase per million fragments (FPKM)

Gene ID	Gene description	Gene name	FPKM ^α			Log2 (fold change) ^β		FDR ^γ	
			CK	PS-NH ₂	PS-COOH	PS-NH ₂	PS-COOH	PS-NH ₂	PS-COOH
Unigene0086391	NF-kappa-B inhibitor alpha [<i>Ruditapes philippinarum</i>]	NFKBIA	17.34	3.60	12.44	-2.27	-0.48	0.01	1.00
Unigene0014347	interleukin-1 receptor-associated kinase 4-like [<i>Aethina tumida</i>]	IRAK4	52.17	1.18	15.60	-5.47	-1.74	0.02	0.90
Unigene0009386	PREDICTED: tubulin alpha-3 chain-like [<i>Chinchilla lanigera</i>]	TUBA	3.92	1.36	0.96	-1.53	-2.03	0.48	0.05
Unigene0066643	PREDICTED: tubulin beta chain, partial [<i>Columba livia</i>]	TUBB	8.07	0.50	7.48	-4.02	-0.11	0.02	1.00
Unigene0043181	cathepsin L [<i>Meretrix meretrix</i>]	CTSL	77.58	16.45	88.77	-2.24	0.19	0.01	1.00
Unigene0001881	PREDICTED: alpha-2 adrenergic receptor [<i>Crassostrea gigas</i>]	CCKAR	2.30	19.26	1.25	3.06	-0.88	0.00	0.89
Unigene0101284	PREDICTED: carboxypeptidase A2-like [<i>Crassostrea gigas</i>]	CPA2	0.00	1.90	1.53	10.89	10.58	0.00	0.65

Unigene0 010921	serine protease CFSP3 [<i>Azumapecten farreri</i>]	CELA2	0.00	4.87	7.09	12.25	12.79	0.01	0.43
Unigene0 014649	PREDICTED: phosphoenolpyruvate carboxykinase, cytosolic [GTP] isoform X2 [<i>Crassostrea gigas</i>]	PCK1	8.18	24.98	6.25	1.61	-0.39	0.00	1.00
Unigene0 056199	PREDICTED: acyl-CoA desaturase-like isoform X2 [<i>Lingula anatina</i>]	SCD-1	13.38	27.12	19.71	1.02	0.56	0.01	1.00
Unigene0 016927	PREDICTED: fatty acid- binding protein, intestinal isoform X2 [<i>Crassostrea gigas</i>]	FABP3	5.73	33.23	11.13	2.54	0.96	0.02	1.00
Unigene0 072869	PREDICTED: ATP- binding cassette sub-family A member 1-like, partial [<i>Saccoglossus kowalevskii</i>]	ABCA1	0.41	2.03	0.53	2.32	0.39	0.02	1.00

^α The FPKM represents the gene expression by normalizing the read counts in transcript.

^β Log₂ (fold change) represents the fold change of gene levels in the PS-NH₂ and PS-COOH groups relative to the control group, respectively.

^γ FDR, the false discovery rate, represents the corrected *P*-value of gene levels in the PS-NH₂ and PS-COOH groups relative to the control group.

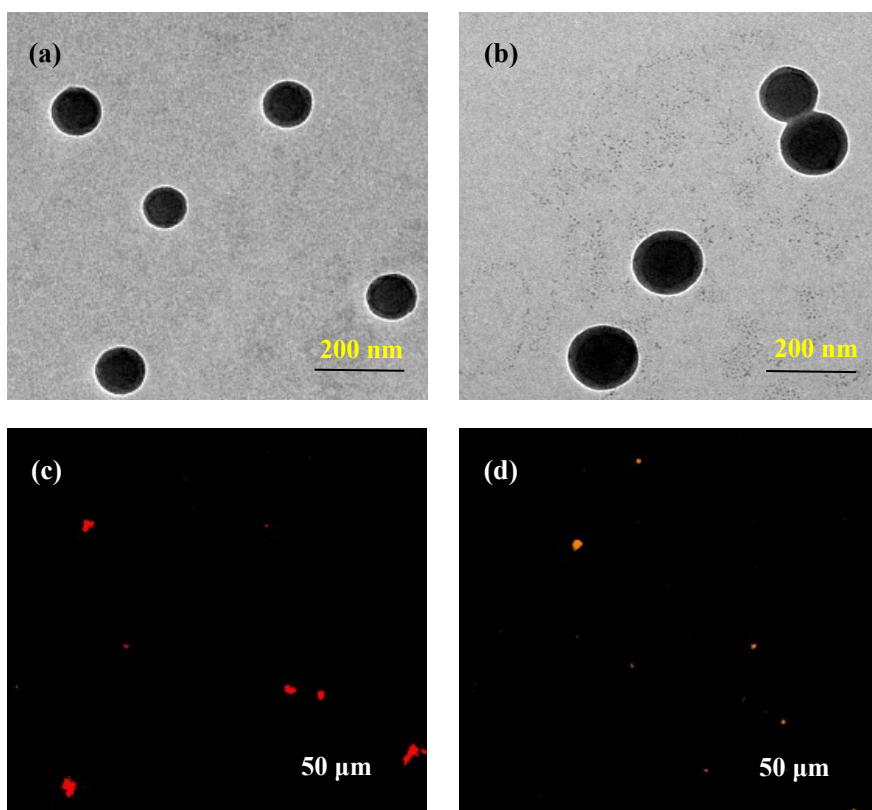


Fig. S1. TEM images of (a) PS-NH₂ and (b) PS-COOH. Fluorescent images of (c) PS-NH₂ and (d) PS-COOH. The NPs were suspended in Milli-Q water (mQW). These data were previously reported by Luan et al.³⁹

┌

Fig. S2. A schematic diagram for the exposure experiment design and sampling protocols. After a 7-day exposure, two clams were randomly selected from each beaker to assess the filtration rate and oxygen consumption rate. Three of clams in each beaker were dissected to excise digestive glands and hemolymph for further analysis of toxic mechanisms of NPs on energy homeostasis and immunomodulation of clams. The weight of shell and soft tissue were measured to calculate the conditional index and water content.

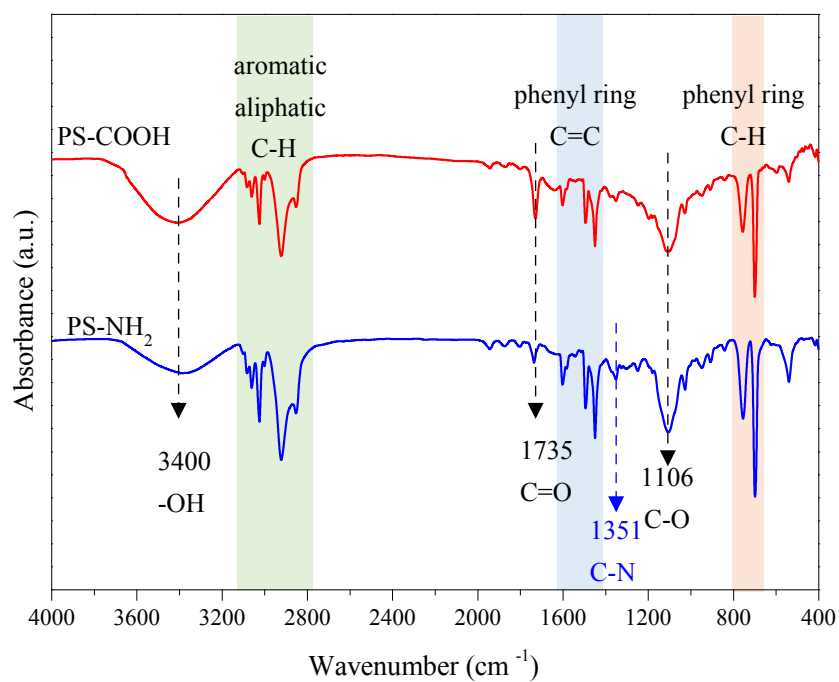


Fig. S3. The spectra of PS-NH₂ and PS-COOH determined using Fourier transformed infrared spectroscopy (FTIR). The shaded parts represent the characteristic peaks of polystyrene polymer. The peaks presented in both of PS-NH₂ and PS-COOH was labeled with black arrows, whereas the characteristic peak only presented in PS-NH₂ was marked with blue arrows.

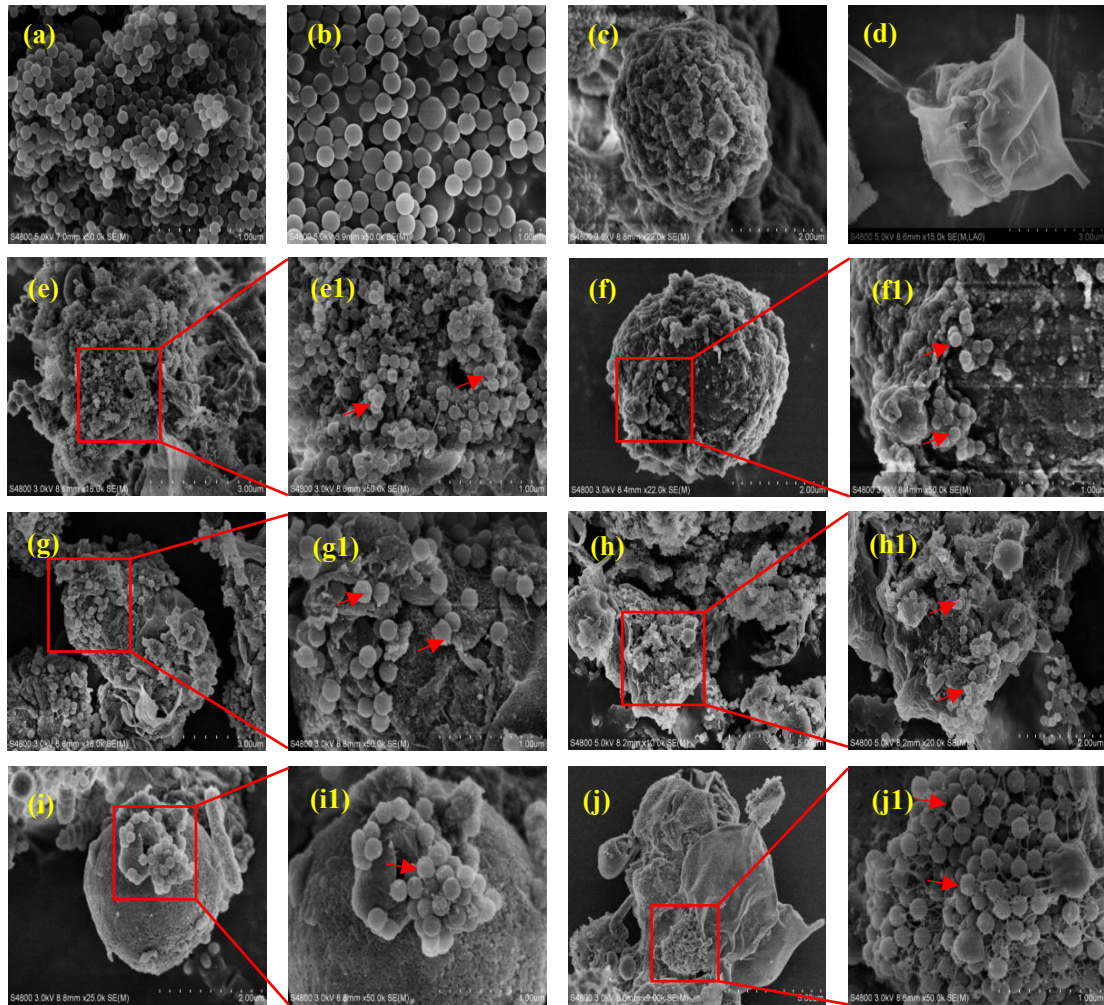


Fig. S4. SEM images of (a) PS-NH₂, (b) PS-COOH, (c) microalgae *I. zhanjiangensis* and (d) *C. meülleri*. The interaction between PS-NH₂ and (e) the mixed algae solution of *C. meülleri* and *I. zhanjiangensis* (1: 1, v/v) (f) microalgae *I. zhanjiangensis*, and (g) *C. meülleri*. The interaction of PS-COOH with (h) the mixed algae solution of *C. meülleri* and *I. zhanjiangensis* (1: 1, v/v) (i) microalgae *I. zhanjiangensis* and (j) *C. meülleri*. The concentration of PS-NH₂ or PS-COOH was 2 mg L⁻¹. The density of microalgae was 2 × 10⁵ cells mL⁻¹. The algae were incubated in an illumination incubator for 24 h at 25 °C under a 12: 12 h light: dark cycle. The panels (e1-g1) show the enlarged regions from the red frames in the panels (e-g). The red arrows indicate the NPs adsorbed on the surface of algae.

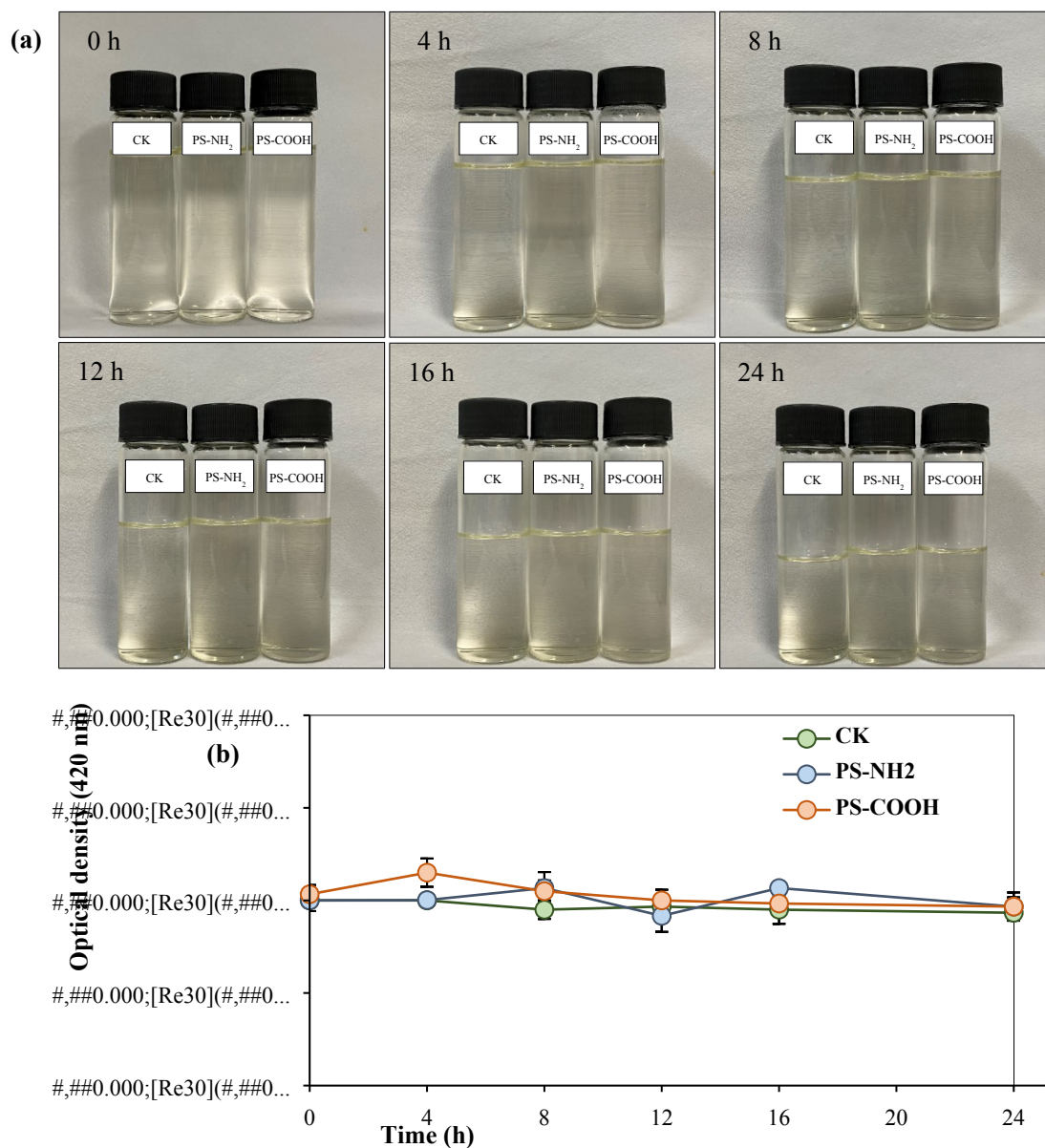


Fig. S5. Images of (a) microalgae *I. zhanjiangensis* (CK), mixed solution of *I. zhanjiangensis* and PS-NH₂ and PS-COOH at 0, 4, 8, 12, 16, 24 h. (b) Effect of PS-NH₂ and PS-COOH on the suspension stability of microalgae *I. zhanjiangensis*. The concentration of PS-NH₂ or PS-COOH was 2 mg L⁻¹. The density of microalgae was 2 × 10⁵ cells mL⁻¹. The algae were incubated in an illumination incubator for 24 h at 25 °C under a 12: 12 h light: dark cycle. There was no significant different of OD value between CK and PS-NH₂/PS-COOH (Duncan's multiple-comparison test, $n = 3$, $P > 0.05$). The error bars represent the standard deviation of the three replicates in each treatment.

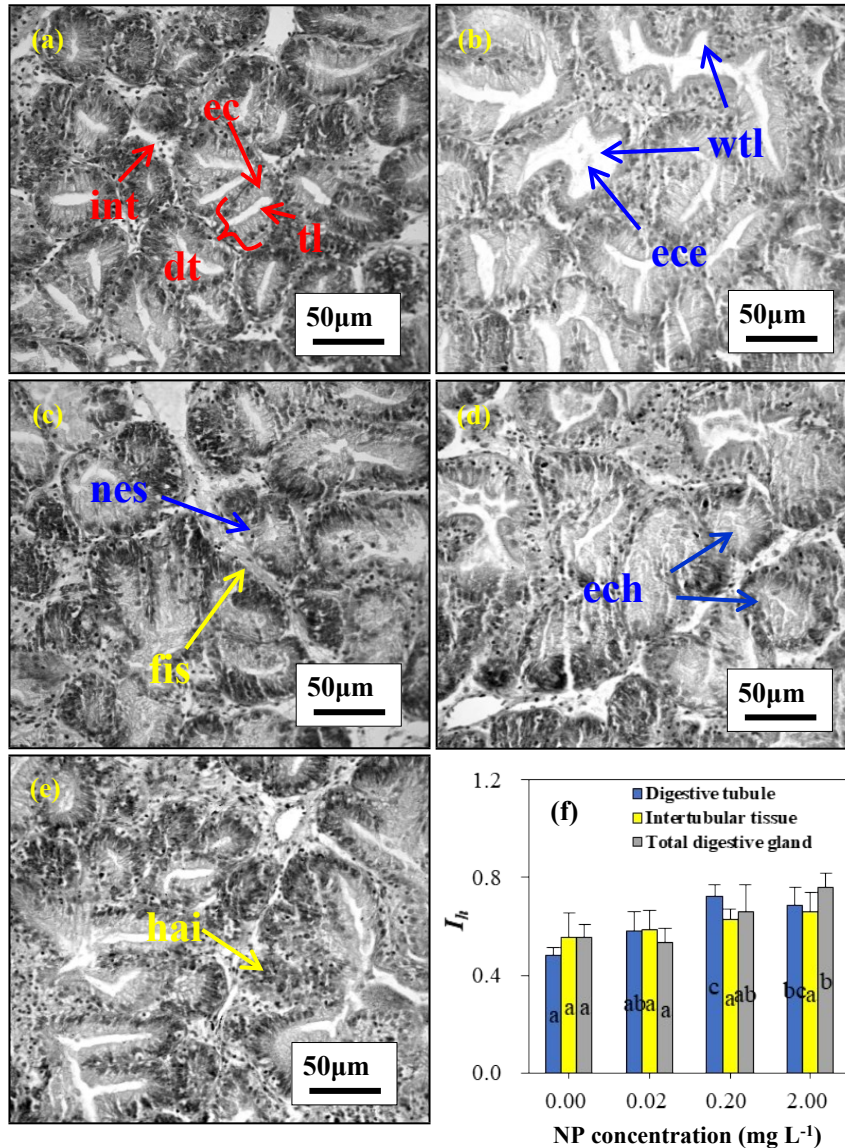


Fig. S6. The histological observations of clam digestive glands. (a) Control digestive glands without PS-COOH exposure, (b-e) pathological digestive glands exposed with PS-COOH at 2 mg L⁻¹. The red arrows indicate the structure of digestive glands, including digestive tubule (dt), epithelial cell (ec), tubule lumen (tl), and intertubular tissues (int). The blue arrows indicate the digestive tubule lesions, including widening of the tubular lumen (wtl), epithelial cell exfoliation (ece), epithelial cell hypertrophy (ech), and necrosis (nes). The yellow arrows indicate the intertubular tissue lesions, including haemocytosis (hai) and fibrosis (fis). (f) Histopathological condition indices (I_h) of the clam digestive glands, which were calculated according to the method described by Costa et al.³⁸ Different small letters indicate significant difference between different concentrations of PS-COOH (Duncan's multiple-comparison test, $n = 3$, $P < 0.05$). The error bars represent the standard deviation of the three replicates in each treatment.

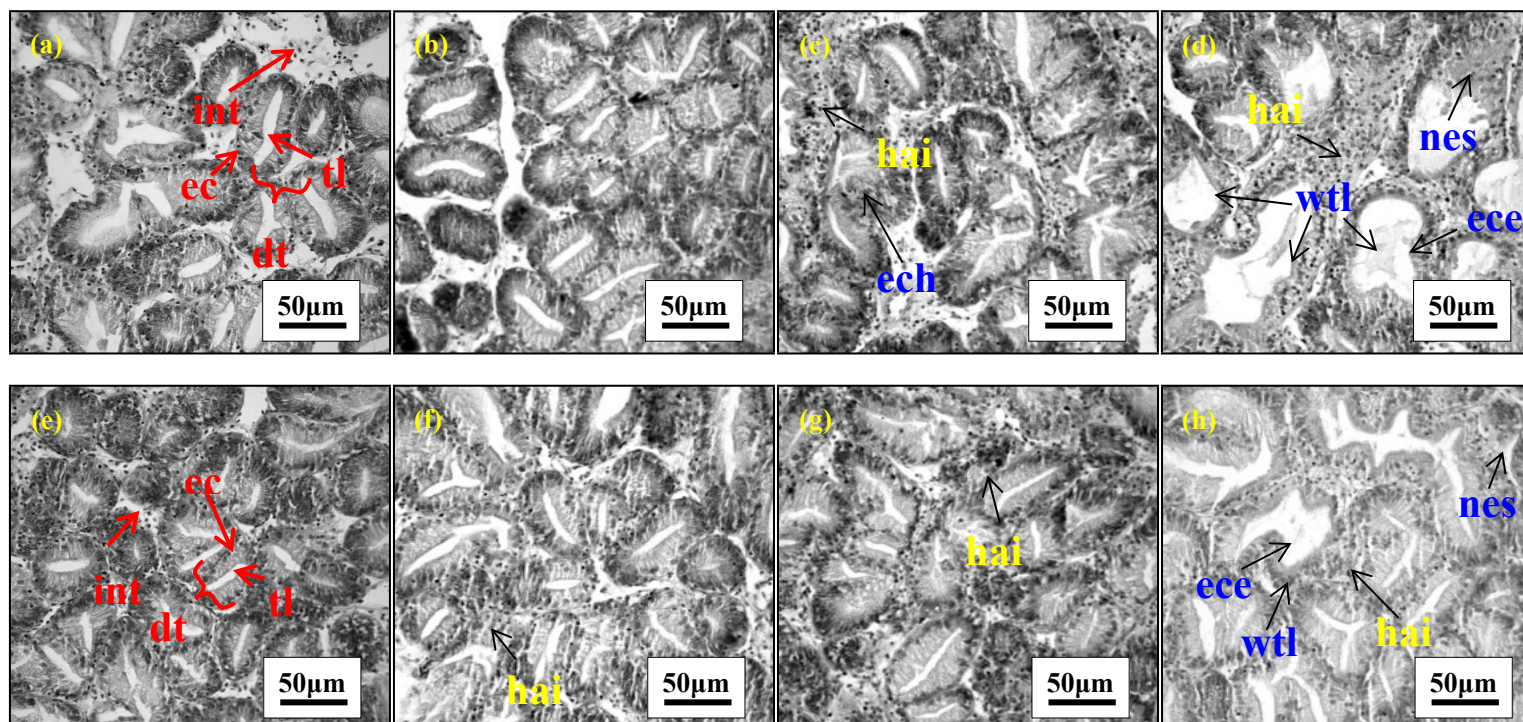


Fig. S7. The histological observations of clam digestive glands. (a) Control digestive glands without PS-NH₂ exposure, (b-d) pathological digestive glands exposed with PS-NH₂ at 0.02, 0.2, and 2 mg L⁻¹, respectively. (e) Control digestive glands without PS-COOH exposure, (f-h) pathological digestive glands exposed with PS-COOH at 0.02, 0.2, and 2 mg L⁻¹, respectively.

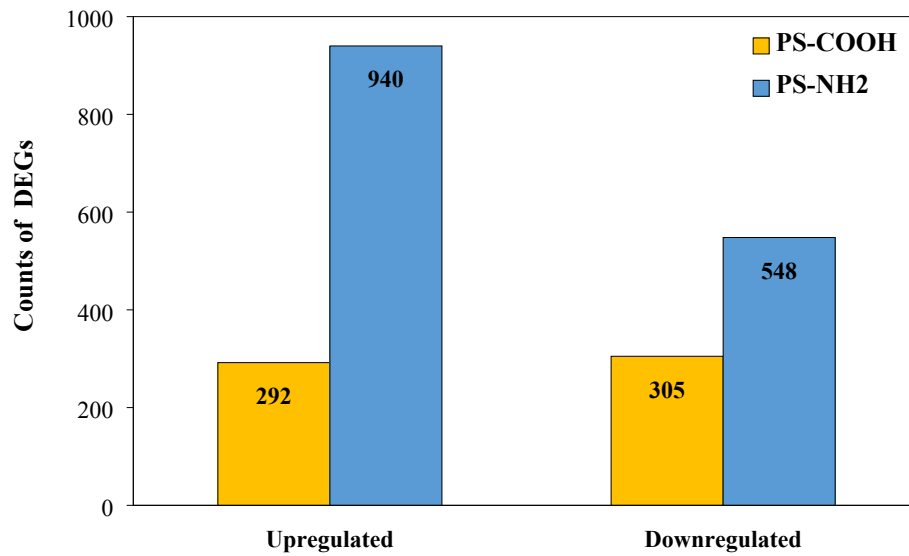


Fig. S8. The counts of downregulated and upregulated differentially expressed genes (DEGs) with absolute values of \log_2 (fold change) > 1 and false discovery rate (FDR) ≤ 0.05 in the clams exposed to 2 mg L^{-1} PS-NH₂ and PS-COOH.

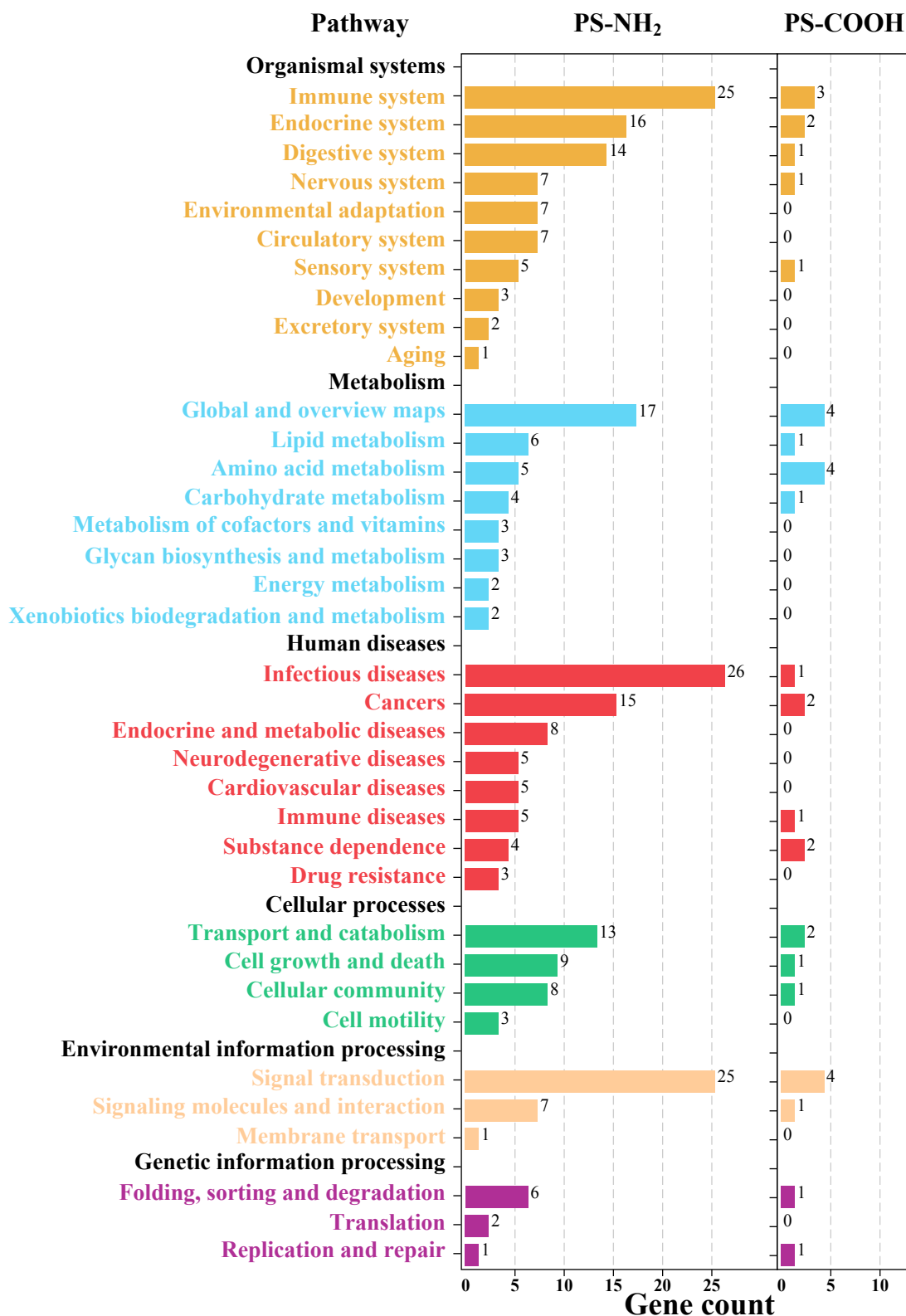


Fig. S9. Significantly enriched Kyoto Encyclopedia of Genes and Genomes (KEGG) pathways of differentially expressed genes (DEGs) in the clam digestive glands exposed to 2 mg L⁻¹ PS-NH₂ and PS-COOH. The color and number of columns represent the KEGG term and the count of DEGs, respectively.

Reference

1. L. M. Hernandez, N. Yousefi and N. Tufenkji, Are there nanoplastics in your personal care products?, *Environ. Sci. Tech. Lett.*, 2017, 4, 280-285.
2. X. Wang, H. Zheng, J. Zhao, X. X. Luo, Z. Y. Wang and B. S. Xing, Photodegradation elevated the toxicity of polystyrene microplastics to grouper (*Epinephelus moara*) through disrupting hepatic lipid homeostasis, *Environ. Sci. Technol.*, 2020, 54, 6202-6212.
3. R. Lenz, K. Enders and T. G. Nielsen, Microplastic exposure studies should be environmentally realistic, *Proc. Natl. Acad. Sci. USA*, 2016, 113, E4121-E4122.
4. T. Gardon, C. Reisser, C. Soyeux, V. Quillien and G. Le Moullac, Microplastics affect energy balance and gametogenesis in the pearl oyster *Pinctada margaritifera*, *Environ. Sci. Technol.*, 2018, 52, 5277-5286.
5. R. Sussarellu, M. Suquet, Y. Thomas, C. Lambert, C. Fabioux, M. E. J. Pernet, N. Le Goic, V. Quillien, C. Mingant, Y. Epelboin, C. Corporeau, J. Guyomarch, J. Robbens, I. Paul-Pont, P. Soudant and A. Huvet, Oyster reproduction is affected by exposure to polystyrene microplastics, *Proc. Natl. Acad. Sci. USA*, 2016, 113, 2430-2435.
6. Q. Zhang, Q. Qu, T. Lu, M. J. Ke, Y. C. Zhu, M. Zhang, Z. Y. Zhang, B. B. Du, X. L. Pan, L. W. Sun and H. F. Qian, The combined toxicity effect of nanoplastics and glyphosate on *Microcystis aeruginosa* growth, *Environ. Pollut.*, 2018, 243, 1106-1112.
7. G. Liu, R. F. Jiang, J. You, D. C. G. Muir and E. Y. Zeng, Microplastic impacts on microalgae growth: Effects of size and humic acid, *Environ. Sci. Technol.*, 2020, 54, 1782-1789.
8. T. T. S. de Oliveira, I. Andreu, M. C. Machado, G. Vimbela, A. Tripathi and A. Bose, Interaction of cyanobacteria with nanometer and micron sized polystyrene particles in marine and fresh water, *Langmuir*, 2020, 36, 3963-3969.
9. C. D. Torre, E. Bergami, A. Salvati, C. Faleri, P. Cirino, K. A. Dawson and I. Corsi, Accumulation and embryotoxicity of polystyrene nanoparticles at early

- stage of development of sea urchin embryos *Paracentrotus lividus*, *Environ. Sci. Technol.*, 2014, 48, 12302-12311.
10. C. B. Jeong, H. M. Kang, Y. H. Lee, M. S. Kim, J. S. Lee, J. S. Seo, M. Wang and J. S. Lee, Nanoplastic ingestion enhances toxicity of persistent organic pollutants (POPs) in the monogonont rotifer *Brachionus koreanus* via multixenobiotic resistance (MXR) disruption, *Environ. Sci. Technol.*, 2018, 11411-11418.
 11. W. Lin, R. F. Jiang, Y. X. Xiong, J. Y. Wu, J. Q. Xu, J. Zheng, F. Zhu and G. F. Ouyang, Quantification of the combined toxic effect of polychlorinated biphenyls and nano-sized polystyrene on *Daphnia magna*, *J. Hazard. Mater.*, 2019, 364, 531-536.
 12. O. O. Fadare, B. Wan, L. H. Guo, Y. Xin, W. P. Qin and Y. Yang, Humic acid alleviates the toxicity of polystyrene nanoplastic particles to *Daphnia magna*, *Environ. Sci.: Nano*, 2019, 6, 1466-1477.
 13. I. Varo, A. Perini, A. Torreblanca, Y. Garcia, E. Bergami, M. L. Vannuccini and I. Corsi, Time-dependent effects of polystyrene nanoparticles in brine shrimp *Artemia franciscana* at physiological, biochemical and molecular levels, *Sci. Total Environ.*, 2019, 675, 570-580.
 14. E. G. Xu, R. S. Cheong, L. Liu, L. M. Hernandez, A. Azimzada, S. Bayen and N. Tufenkji, Primary and secondary plastic particles exhibit limited acute toxicity but chronic effects on *Daphnia magna*, *Environ. Sci. Technol.*, 2020, 54, 6859-6868.
 15. A. Wegner, E. Besseling, E. M. Foekema, P. Kamermans and A. A. Koelmans, Effects of nanopolystyrene on the feeding behavior of the blue mussel (*Mytilus edulis* L.), *Environ. Toxicol. Chem.*, 2012, 31, 2490-2497.
 16. L. Canesi, C. Ciacci, R. Fabbri, T. Balbi, A. Salis, G. Damonte, K. Cortese, V. Caratto, M. P. Monopoli, K. Dawson, E. Bergami and I. Corsi, Interactions of cationic polystyrene nanoparticles with marine bivalve hemocytes in a physiological environment: Role of soluble hemolymph proteins, *Environ. Res.*, 2016, 150, 73-81.

17. M. Al-Sid-Cheikh, S. J. Rowland, K. Stevenson, C. Rouleau, T. B. Henry and R. C. Thompson, Uptake, whole-body distribution, and depuration of nanoplastics by the scallop *Pecten maximus* at environmentally realistic concentrations, *Environ. Sci. Technol.*, 2018, 52, 14480-14486.
18. C. Gonzalez-Fernandez, K. Tallec, N. Le Goic, C. Lambert, P. Soudant, A. Huvet, M. Suquet, M. Berchel and I. Paul-Pont, Cellular responses of Pacific oyster (*Crassostrea gigas*) gametes exposed in vitro to polystyrene nanoparticles, *Chemosphere*, 2018, 208, 764-772.
19. K. Tallec, A. Huvet, C. Di Poi, C. Gonzalez-Fernandez, C. Lambert, B. Petton, N. Le Goic, M. Berchel, P. Soudant and I. Paul-Pont, Nanoplastics impaired oyster free living stages, gametes and embryos, *Environ. Pollut.*, 2018, 242, 1226-1235.
20. W. S. Zhou, Y. Han, Y. Tang, W. Shi, X. Y. Du, S. G. Sun and G. X. Liu, Microplastics aggravate the bioaccumulation of two waterborne veterinary antibiotics in an edible bivalve species: Potential mechanisms and implications for human health, *Environ. Sci. Technol.*, 2020, 54, 8115-8122.
21. Z. L. Li, C. H. Feng, Y. H. Wu and X. Y. Guo, Impacts of nanoplastics on bivalve: Fluorescence tracing of organ accumulation, oxidative stress and damage, *J. Hazard. Mater.*, 2020, 392, 122418.
22. N. R. Brun, B. E. V. Koch, M. Varela, W. J. G. M. Peijnenburg, H. P. Spaink and M. G. Vijver, Nanoparticles induce dermal and intestinal innate immune system responses in zebrafish embryos, *Environ. Sci.: Nano*, 2018, 5, 904-916.
23. W. S. Lee, H. J. Cho, E. Kim, Y. H. Huh, H. J. Kim, B. Kim, T. Kang, J. S. Lee and J. Jeong, Bioaccumulation of polystyrene nanoplastics and their effect on the toxicity of Au ions in zebrafish embryos, *Nanoscale*, 2019, 11, 3173-3185.
24. H. X. Gu, S. X. Wang, X. H. Wang, X. Yu, M. H. Hu, W. Huang and Y. J. Wang, Nanoplastics impair the intestinal health of the juvenile large yellow croaker *Larimichthys crocea*, *J. Hazard. Mater.*, 2020, 397, 122773.
25. C. J. Moore, S. L. Moore, M. K. Leecaster and S. B. Weisberg, A comparison of plastic and plankton in the North Pacific Central Gyre, *Mar. Pollut. Bull.*, 2001,

- 42, 1297-1300.
26. J. Reisser, J. Shaw, C. Wilcox, B. D. Hardesty, M. Proietti, M. Thums and C. Pattiaratchi, Marine plastic pollution in waters around Australia: Characteristics, concentrations, and pathways, *PLoS One*, 2013, 8, e80466.
 27. M. Eriksen, N. Maximenko, M. Thiel, A. Cummins, G. Lattin, S. Wilson, J. Hafner, A. Zellers and S. Rifman, Plastic pollution in the South Pacific subtropical gyre, *Mar. Pollut. Bull.*, 2013, 68, 71-76.
 28. V. Fischer, N. O. Elsner, N. Brenke, E. Schwabe and A. Brandt, Plastic pollution of the Kuril–Kamchatka Trench area (NW pacific), *Deep-Sea Res. Pt. II*, 2015, 111, 399-405.
 29. Y. B. Li, Z. B. Lu, H. Y. Zheng, J. Wang and C. Chen, Microplastics in surface water and sediments of Chongming Island in the Yangtze Estuary, China, *Environ. Sci. Eur.*, 2020, 32, 2-12.
 30. M. Narmatha Sathish, K. Immaculate Jeyasanta and J. Patterson, Monitoring of microplastics in the clam *Donax cuneatus* and its habitat in Tuticorin coast of Gulf of Mannar (GoM), India, *Environ. Pollut.*, 2020, 266, 115219.
 31. J. Patterson, K. I. Jeyasanta, N. Sathish, J. K. P. Edward and A. M. Booth, Microplastic and heavy metal distributions in an Indian coral reef ecosystem, *Sci. Total Environ.*, 2020, 744, 140706.
 32. T. Wang, M. H. Hu, L. L. Song, J. Yu, R. J. Liu, S. X. Wang, Z. F. Wang, I. M. Sokolova, W. Huang and Y. J. Wang, Coastal zone use influences the spatial distribution of microplastics in Hangzhou Bay, China, *Environ. Pollut.*, 2020, 266, 115137.
 33. A. Faruk Cullu, V. Z. Sonmez and N. Sivri, Microplastic contamination in surface waters of the Kucukcekmece Lagoon, Marmara Sea (Turkey): Sources and areal distribution, *Environ. Pollut.*, 2020, 268, 115801-115801.
 34. J. Tang, Z. J. Wu, L. Wan, W. Q. Cai, S. Q. Chen, X. J. Wang, J. Luo, Z. Zhou, J. M. Zhao and S. J. Lin, Differential enrichment and physiological impacts of ingested microplastics in scleractinian corals in situ, *J. Hazard. Mater.*, 2020, 404, 124205-124205.

35. Y. Bouallegui, R. Ben Younes, H. Bellamine and R. Oueslati, Histopathological indices and inflammatory response in the digestive gland of the mussel *Mytilus galloprovincialis* as biomarker of immunotoxicity to silver nanoparticles, *Biomarkers*, 2017, 1-11.
36. T. L. Rocha, S. M. T. Sabóia-Morais and M. J. Bebianno, Histopathological assessment and inflammatory response in the digestive gland of marine mussel *Mytilus galloprovincialis* exposed to cadmium-based quantum dots, *Aquat. Toxicol.*, 2016, 177, 306-315.
37. N. Cuevas, I. Zorita, P. M. Costa, J. Franco and J. Larreta, Development of histopathological indices in the digestive gland and gonad of mussels: integration with contamination levels and effects of confounding factors, *Aquat. Toxicol.*, 2015, 162, 152-164.
38. P. M. Costa, S. Carreira, M. H. Costa and S. Caeiro, Development of histopathological indices in a commercial marine bivalve (*Ruditapes decussatus*) to determine environmental quality, *Aquat. Toxicol.*, 2013, 126, 442-454.
39. L. P. Luan, X. Wang, H. Zheng, L. Q. Q. Liu, X. X. Luo and F. M. Li, Differential toxicity of functionalized polystyrene microplastics to clams (*Meretrix meretrix*) at three key development stages of life history, *Mar. Pollut. Bull.*, 2019, 139, 346-354.